Effect of precursor of refinement Y211 on the superconductivity and structural of Y257 superconductors

Thitipong Kruaehong[a,*], Supphadate Sujinnapram[b], Tunyanop Nilkamjon[c], Sermsuk Ratreng[c], Pongkaew Udomsamuthirun[c]

[a] Department of industrial electric, Faculty of Science and Technology, Suratthani Rajabhat University, Suratthani, 84100 Thailand
[b] Department of Physics, Faculty of Liberal Arts and Science, Kasetsart University, Kamphaeng Saen Campus, Nakhon Pathom, 73140 Thailand
[c] Prasarnmit Physics Research, Department of Physics, Faculty of Science, Srinakharinwirot University, Bangkok, 10110 Thailand

***Corresponding Author:** thitipong.kru@sru.ac.th
https://doi.org/10.55674/jmsae.v12i3.247682

Received: 21 February 2022 | **Revised:** 22 March 2022 | **Accepted:** 19 July 2023| **Available online:** 1 September 2023

Abstract

Y211 was added to the Y257 superconducting material at concentrations of 0, 0.10, and 0.20 mol using a solid-state reaction synthesis method. As the concentration of Y211 increased, both the onset critical temperature and the offset critical temperature decreased. The synthesized samples contained a combination of superconducting and non-superconducting compounds. The superconducting compound exhibited an orthorhombic structure with the Pmmm space group. Additionally, three different types of non-superconducting compounds were identified in the samples. The percentage of non-superconducting compounds increased with the addition of Y211. The surface morphology revealed heterogeneous elements and a random distribution of grain sizes. The samples contained Y, Ba, Cu, and O elements without any detectable impurities.

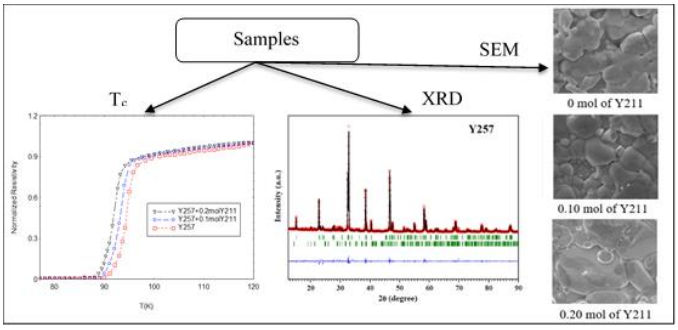

Keywords: Y257 superconductor; Non-superconducting compound; Y211 superconductor

Introduction

In the past three decades, Y-based superconductors have been discovered in various groups [1 – 2]. The key findings of these discoveries were the novel critical temperature values and crystal structures. The conventional Y-based superconducting material, Y123 ($YBa_2Cu_3O_{7-x}$), was the first superconductor found in 1987, exhibiting a critical temperature above 90 K [3]. Numerous researchers have conducted studies and advancements to enhance the superconducting properties of Y-based materials for various fields of application, including superconducting magnetic bearings [4], superconducting electric motors [5], magnetic separation devices [6], non-contact transport systems [7], and flywheel energy storage systems [8], among others. In 2013, Kruaehong [9] successfully synthesized bulk Y-based superconductors of Y257 through a solid-state reaction method. High-purity powders of Y_2O_3 (99.99% purity), $BaCO_3$ (99.98% purity), and CuO (99.99% purity) were used as starting materials. The powders were calcined and sintered at 1,223 K for 24 h, followed by annealing at 773 K for 12 h in air, and then cooled to room temperature. The critical temperature of the samples was measured using a four-probe setup, and the crystal structure was investigated using the powder X-ray diffraction technique with CuK_α radiation. The X-ray diffraction patterns were analyzed using the FULLPROF software refinement program [10]. The critical temperature of the samples was measured to be 94.97 K, and the lattice parameters of the superconducting samples were found to be a = 3.8108 Å, b = 3.8544 Å, and c = 26.4967 Å, with the Pmmm space group. The non-superconducting samples exhibited two different space groups: Pccm with a = 12.9770 Å, b = 20.54780 Å, and

c = 11.3530 Å; and Im-3m with *a* = 18.2104 Å, *b* = 18.2104 Å, and *c* = 18.2104 Å. The critical temperature of Y123 and Y257 remained close to each other. In recent years, a new Y-based superconductor, Y358 ($Y_3Ba_5Cu_8O_{18-x}$), has been discovered with a critical temperature above 102 K [11]. The lattice parameters of Y358 are *a* = 3.888 Å, *b* = 3.823 Å, and *c* = 31.013 Å, with Pmm2 symmetry, respectively. The critical temperature is an important physical property requirement that is given first consideration for applications. It is well-known that the second phase in Y123, Y211 (Y_2BaCuO_5), can enhance the physical properties, such as increasing the critical current density (J_c) and high magnetic field (H_c). The effect of Y211 in Y123 composites has been studied by numerous research groups [12 – 14].

In this present work, we investigated the effect of doping the Y257 superconductors with the non-superconducting compound (Y211, Y_2BaCuO_5) at ratios of 0, 0.10, and 0.20 mol, respectively. The critical temperature was determined using d.c. electrical four-probe measurements. Structural analysis was performed using powder X-ray diffraction, while surface morphology and elemental analysis were investigated using EDX mapping techniques.

Materials and Methods

High-purity powders of Y_2O_3, $BaCO_3$, and CuO (all with a purity of 99.99%) were used as starting materials. The raw materials for Y257 and Y211 were mixed in different atomic ratios of 2:5:7 and 2:1:1, respectively. The mixture of Y257 and Y211 powders was calcined at 1,223 K for 24 h. The calcination process was repeated twice with intermediate grinding of the powders. The black powder of Y257 and the green powder of Y211 were obtained. Y211 in quantities of 0 mol, 0.10 mol, and 0.20 mol were mixed with the black powder of Y257. The mixed powders were then calcined at 1,223 K and kept at that temperature for 24 h. A hydraulic machine was used to press the powders into pellets with dimensions of approximately 30 mm in diameter and 5 mm in thickness, applying a pressure of 2,000 psi. The bulk samples were sintered at 1,223 K for 24 h and subsequently annealed at 773 K with oxygen doping in an air environment.

Electrical resistivity and powder X-ray diffraction techniques were used to investigate the superconductivity and crystal structure of the samples. The critical temperature was determined by measuring the onset critical temperature (T_c onset) and the offset critical temperature (T_c offset). The resistivity as a function of temperature was measured using a four-probe setup within the temperature range of 77 – 120 K, with the system cooled down using liquid nitrogen. The crystal structure analysis was performed using powder X-ray diffraction. The data were collected using a D8 Advance Discovery diffractometer with CuK_α as the X-ray source, producing a monochromatic beam with a wavelength of 1.5416 Å. The 2θ angle was examined in the range of 10° – 90°, with a scan speed of 3.40° min and an increment angle of 0.02° at room temperature. The percentage composition of the samples, lattice parameters, and space group corresponding to the phase composition were determined using the Rietveld refinement method. The surface characteristics and elemental analysis were carried out using the FEI Quanta 400.

Results and Discussions

The resistivity versus temperature measurements of the bulk Y257 and Y211 composite were performed using a d.c. electrical resistivity measurement setup, with a constant d.c. current of 3.18 mA m^{-2} and temperature measurement conducted using a type K thermocouple. The results are shown in Fig. 1. The temperature was cooled down from room temperature (around 300 K) to 77 K using liquid nitrogen. Temperature measurements were taken at intervals of 77 K up to 120 K. The offset critical temperature (T_c offset) was defined as the temperature at which the resistivity reached zero. The T_c offset values were measured as 86.35 K, 85.63 K, and 84.23 K for Y257, Y257 + 0.10 mol, and Y257 + 0.20 mol, respectively. The onset critical temperature (T_c onset) is defined as the temperature at which a significant change occurs. The T_c onset values were measured as 93.98 K, 93.62 K, and 92.13 K for Y257, Y257 + 0.10 mol, and Y257+0.20 mol, respectively. The presence of the non-superconducting compound Y211 had an effect

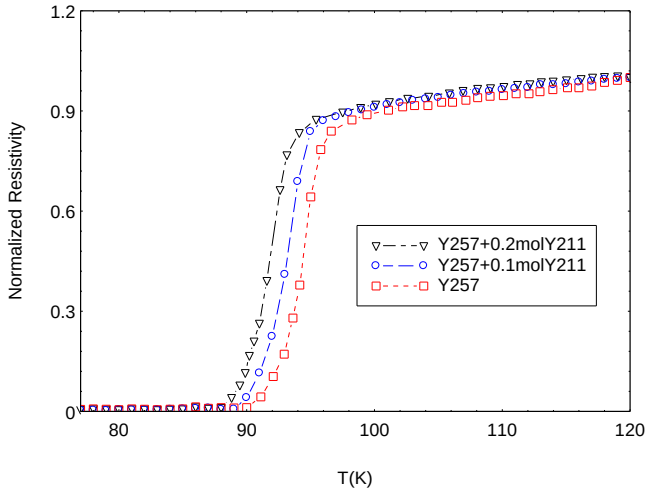

Fig. 1 Graph plot between resistivity versus temperature of Y257 and Y211 composite.

on the critical temperature of Y257. Both the T_c offset, and T_c onset showed a decrease. In 2000, Jezowski et al. [15] reported that Y211 also causes increased phonon and quasi-particle scattering in the crystal structure, resulting in poor grain connectivity and a decrease in critical temperature when Y211 is added to the samples.

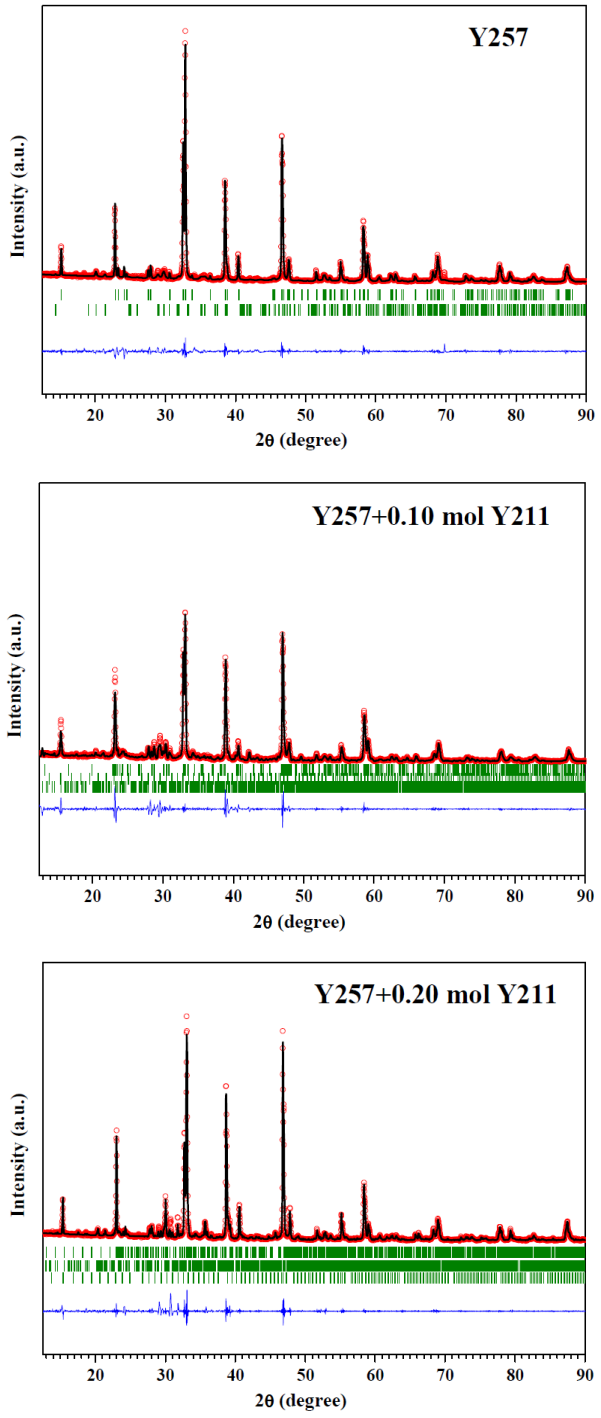

Fig. 2 XRD pattern of Y257 and Y257+Y211 superconductors.

The XRD patterns of the Y257 and Y211 composite profiles are shown in Fig. 2. The Rietveld refinement method was used to determine the characteristics of the orthorhombic structure, phase compositions, and space group. Our samples exhibit a polycrystalline nature with varying peak intensities. The raw XRD data was analyzed using the High X-Pert Scopus program to search for matches in the ICDD database. Most of the peaks corresponded to the spectrum of the superconducting compound, while other peaks corresponded to the non-superconducting compound. The percentages of the superconducting and non-superconducting spectra were calculated and are shown in Table 1. The pure Y257 sample exhibited the highest percentage of the superconducting compound. With the addition of Y211, the percentage of the superconducting phase decreased. The pure Y257 sample also showed the presence of the non-superconducting phase, with Y211 constituting approximately 20% of the sample. The occurrence of non-superconducting phases was observed in the samples. With the addition of Y211, two non-superconducting compounds, $BaCuO_2$ and $Ba_2Cu_3O_6$, were observed. The superconducting compound exhibited an orthorhombic structure with Pmmm symmetry group. Y211 and $Ba_2Cu_3O_6$ also showed an orthorhombic structure with Pbnm and Pccm space groups, respectively, while $BaCuO_2$ had a cubic structure with Im-3m space group. The lattice parameters of the superconducting compound indicating the orthorhombic structure are shown in Table 2. The lattice parameters of the non-superconducting compounds are shown in Table 3.

In Fig. 3, the SEM micrographs of the samples are shown. The samples were examined at high magnifications of ×5,000. The SEM images captured the different morphologies of the a and b planes. The pure Y257 sample exhibited a crack-free surface with large pores. However, with the addition of Y211, the presence of pores and cracks on the surface decreased. All three samples showed variations in grain size and orientation, indicating a lack of uniformity. The interpretation of the SEM images aligns with the findings reported by Imagawa and Shiohara [16] in 1996. The SEM images were obtained using backscattered electron imaging. The elementary analysis was conducted using Energy Dispersive X-ray Spectroscopy. The results showed that the samples contained varying amounts of Y, Ba, Cu, and O, without any impurities. The scale bar in the SEM analysis was set to 10 μm and was used to measure the results shown in the micrographs. The addition of Y211 improved the grain size of the Y257 superconductors, with higher concentrations of Y211 resulting in larger grain sizes.

Table 1 The percentage of composite compound.

Samples	Superconducting Compound	Non-superconducting Compound		
		(Y_2BaCuO_5), Pbnm	$BaCuO_2$, Im-3m	$Ba_2Cu_3O_6$, Pccm
Y257	80	20	-	-
Y257+0.10 mol Y211	70	10	5	15
Y257+0.20 mol Y211	65	10	15	10

Table 2 The lattice parameter of the superconducting compound with Pmmm space group.

Samples	Lattice constant		
	a(Å)	*b*(Å)	*c*(Å)
Y257	3.80	3.87	26.55
Y257+0.10 mol Y211	3.80	3.87	26.33
Y257+0.20 mol Y211	3.80	3.88	26.31

Table 3 The lattice parameter of the non-superconducting compound.

Samples	Non-superconducting compound								
	Y211(Y_2BaCuO_5), Pbnm			$BaCuO_2$, Im-3m			$Ba_2Cu_3O_6$, Pccm		
	a(Å)	*b*(Å)	*c*(Å)	*a*(Å)	*b*(Å)	*c*(Å)	*a*(Å)	*b*(Å)	*c*(Å)
Y257	7.20	12.18	5.64	-	-	-	-	-	
Y257+0.10 mol Y211	7.23	12.28	5.70	18.21	18.21	18.21	13.08	20.73	11.12
Y257+0.20 mol Y211	7.23	12.23	5.52	18.41	18.41	18.41	13.01	20.45	11.14

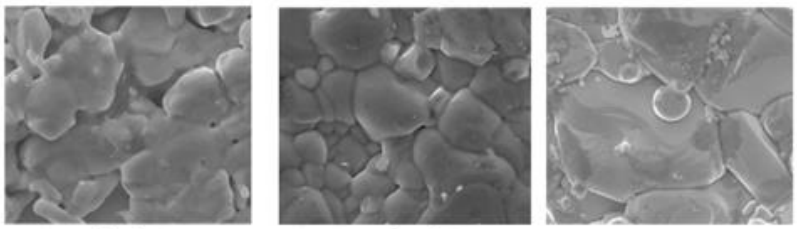

Fig.3 SEM micrographs of Y257 and Y211 composite.

The addition of Y211 to Y257 affected the critical temperature values of T_c offset and T_c onset. Both T_c values shifted to lower temperatures. Furthermore, the addition of Y211 resulted in a decrease in the c-lattice parameter and a reduction in the proportion of superconducting compound in pure Y257. The presence of Y211 led to an improvement in surface smoothness and density, as well as the formation of larger grain sizes. The presence of large grain sizes can result in a decrease in weak links and an increase in critical current density [17], as well as the trapping of high critical magnetic fields [18].

Conclusion

The Y257 superconducting material and the Y211 non-superconducting material were synthesized through a solid-state reaction. The samples were calcined and sintered at 1,223 K. The Y211 powder was mixed with the Y257 superconductor in concentrations of 0, 0.10, and 0.20 mol. The resulting pellets of the mixed samples were analyzed using four-probe measurements to determine the critical temperature. The crystal structure of the samples was examined using powder X-ray diffraction, and phase compositions, lattice parameters, and space groups were determined through Rietveld refinement. The addition of

Y211 resulted in a decrease in the critical temperature values of Tc offset (K) and Tc onset. The samples contained two compounds. The first compound was a superconducting compound with an orthorhombic structure and a Pmmm symmetry space group. The second compound was a non-superconducting compound, which had three different types. The first type was Y211, which had an orthorhombic structure with a Pbnm space group. The second type was $BaCuO_2$, which had a cubic structure with an Im-3m space group. Finally, the $Ba_2Cu_3O_6$ compound had an orthorhombic structure with a Pccm space group. The percentage of the superconducting compound decreased with increasing Y211 concentration. The surface morphology exhibited inhomogeneity with random pore distribution and random orientation of grain sizes. The samples were composed of the elements Y, Ba, Cu, and O, and no impurities were detected.

Acknowledgement

Financial support from Department of Mechanical Engineering, Faculty of Engineering and Industrial Technology, Kalasin University.

References

[1] P. Marsh, R.M. Fleming, M.L. Mandich, A.M. Desantolo, J. Kwo, M, Hong, L.J. Martinez-Miranda, Crystal Structure of the 80 K Superconductor $YBa_2Cu_4O_8$, Nature. 334 (1988) 141 − 143.

[2] P. Bordet, C. Chaillout, J. Chenavas, J.L. Hodeau, M. Marezio, J.Karpinski, E. Kaldis, Structure Determination of the New High Temperature Superconductor $Y_2Ba_4Cu_7O_{14+x}$, Nature. 334 (1988) 596 − 598.

[3] K. Wu, J.R. Ashburn, C.J. Torng, P.H. Hor, R.L. Meng, L. Gao, Z.J. Huang, Y.Q. Wang, C.W. Chu, Superconductivity at 93 K in a New Mixed-Phase Y-Ba-Cu-O Compound System at Ambient Pressure, Phys. Rev. Lett. 58 (1987) 908 − 910.

[4] T. Jiqiang, F. Jiancheng, S.G.Shuzhi, Role of superconducting magnetic bearings and active magnetic bearing in attitude control and energy storage flywheel, Physica C. 483(2012) 178 − 185.

[5] O. Hiroyuki, T. Yuichi, Study and electric motor with bulk superconductors in the rotor, Journal of mat Proc and Tech. 108(2001) 148 − 151.

[6] T. Oka, T. Kimura, D. Mimura, H. Fukazawa, S. Fukui, J. Ogawa, T. Sato, M. Ooizumi, K. Yokoyama, M. Tsujimura, T. Terasawa, Magnetic precipitate separation for Ni plating wate liquid using HTS bulk magnet. Physica C. 484 (2013) 325 − 328.

[7] C.W. Smith, P.J. Dolan, Determining transport parameters for superconductor/normal metal point contact at fixed temperature from conductance versus magnetic data, Physica C. 471 (2013) 285 − 289.

[8] Y. Arai, H. Seino, K. Yoshizawa, K. Nagashima, Development of superconducting magnetic bearing with superconducting coil and bulk superconductor for flywheel energy storage system, Physica C. 494 (2013) 250 − 254.

[9] T. Kruaehong, Preparation and Characterization of the new Y257 superconductors, Adv. Mat. Res. 770 (2013) 22 − 25.

[10] J. Rodriguez-Carvajal, Program FULLPROF. Laboratoire Leon Brillouin (CEACNRS), (1991) Version, 3.

[11] A. Aliabadi, A. Farshchi, M. Akhavan, A New Y-based HTSC with Tc above 100 K, Physica C. 469 (2009) 2012 − 2014.

[12] J. Mucha, K. Rogacki, H. Misiorek, A. Jezowski, A. Wisniewski, R. Puzniak, Influence of the Y211 phase on anisotropic transport properties and vortex dynamics of the melt-textured Y123/Y211 composites, Physica C. 470 (2010) S1009 – S1010.

[13] H. Zhang, K. Du, H. Ye, Z.H. Wang, Oxygen diffusion in the ceramic composite of $YBa_2Cu_3O_y$ with Y_2BaCuO_5. Physica C. 386 (2003) 249 – 253

[14] F. Delorme, J.-F. Bardeau, C. Harnois, I. Monot-Laffez, Evidence of oxygen content heterogeneity in TSMTG YBa2Cu3O7-δ/Y2BaCuO5 composites by micro-Raman spectrometry, Physica C. 468 (2008) 388 – 393.

[15] A. Jezowski, K. Rogacki, T. Puig, X. Obradors, Anisotropy of the thermal conductivity of melt-textured Y123/Y211 composite, Physica B. 284 – 288 (2000) 1015 – 1016.

[16] Y. Imagawa, Y. Shiohara, Effect of Precursor Processing on refinement of Y2BaCuO5 in Melt-Processed $YBa_2Cu_3O_{6+x}$ by Unidirectional Solidification, Physica C. 268 (1996) 61 – 70.

[17] K. Nakazato, M. Muralidhar, M.R. Koblischka, M. Murakami, Fabrication of bulk Y-Ba-Cu-O superconductors with high critical current densities through the infiltration-growth process, Cryogenics. 63 (2014) 129 – 132.

[18] F.N. Werfel, U. Floegel-Delor, T. Riedel, B. Goebel, R. Rothfeld, P. Schirrmeister, D. Wippich, Large-scale HTS bulks for magnetic application, Physica C. 484 (2013) 6 – 11.